

Proteomic and genomic characterization of chromatin complexes at a boundary

Alan J. Tackett,¹ David J. Dilworth,^{2,3} Megan J. Davey,¹ Michael O'Donnell,^{1,4} John D. Aitchison,^{2,3} Michael P. Rout,¹ and Brian T. Chait¹

¹The Rockefeller University, New York, NY 10021

²Institute for Systems Biology, Seattle, WA 98103

³University of Alberta, Edmonton, Alberta T6G2H7, Canada

⁴Howard Hughes Medical Institute, The Rockefeller University, New York, NY 10021

We have dissected specialized assemblies on the *Saccharomyces cerevisiae* genome that help define and preserve the boundaries that separate silent and active chromatin. These assemblies contain characteristic stretches of DNA that flank particular regions of silent chromatin, as well as five distinctively modified histones and a set of protein complexes. The complexes consist of at least 15 chromatin-associated

proteins, including DNA pol ϵ , the Isw2-Itc1 and Top2 chromatin remodeling proteins, the Sas3-Spt16 chromatin modifying complex, and Yta7, a bromodomain-containing AAA ATPase. We show that these complexes are important for the faithful maintenance of an established boundary, as disruption of the complexes results in specific, anomalous alterations of the silent and active epigenetic states.

Introduction

Gene expression in eukaryotes is regulated at several different levels. At the level of chromosome structure, the chromatin is organized into regions with different degrees of accessibility to the transcriptional machinery. The more condensed or protected regions of chromatin are relatively inaccessible and so transcriptionally “silent,” whereas “active” regions are more open and accessible (for reviews see Rusche et al., 2003; Vermaak et al., 2003). Specialized boundary zones have been found between certain silent and active regions; these zones prevent the invasion of either region into the other (for reviews see Bi and Broach, 2001; Labrador and Corces, 2002) (Burgess-Beusse et al., 2002). The silent, active and boundary regions all represent stably maintained and heritable epigenetic states of localized chromatin organization. The cell therefore requires machineries that establish, maintain, and ensure the faithful replication of all the epigenetic states on chromosomes. This appears to be accomplished through a coordinated and intricate choreography of protein–DNA complex formation and modification. Strategies for establishing and maintaining the silent and active regions of chromatin include packaging the DNA with appropriately modified histones (Jenuwein and Allis,

2001; Vermaak et al., 2003), the use of energy-driven chromatin remodeling machinery (Becker and Horz, 2002), and the addition of specific chromatin-associated proteins (Meneghini et al., 2003; Rusche et al., 2003; Mizuguchi et al., 2004).

The molecular bases of such epigenetic phenomena have been extensively investigated in the yeast *Saccharomyces cerevisiae*, where the majority of its chromatin is maintained in an active state. Much of the remaining relatively inactive chromatin (estimated ~10% [van Leeuwen et al., 2002]) is concentrated toward the telomeres and at the rRNA-encoding DNA locus. The silent mating type loci (*HML* and *HMR*) are found proximal to the telomeres of chromosome III (Rusche et al., 2003), and are among the best studied examples of epigenetic control. It has been shown that specialized boundary regions serve to isolate the silent chromatin of *HML* and *HMR* from their surrounding active regions (for reviews see Haber, 1998; Dhillon and Kamakaka, 2002) (Bi et al., 1999; Donze et al., 1999; Donze and Kamakaka, 2001; Lieb et al., 2001; Zhang et al., 2002; Ishii and Laemmli, 2003).

Currently, only a limited amount of information is available about proteins that establish, maintain, and replicate these boundary zones or the modification states of the associated histones (Donze et al., 1999; Laloraya et al., 2000; Ishii and Laemmli, 2003; Oki et al., 2004). Although chromatin immunoprecipitation (ChIP) techniques have allowed significant progress in the study of individual protein–DNA interactions, techniques for the overall analysis of the epigenetic states of chromatin are still in their infancy. In particular, a current

Correspondence to Brian T. Chait: chait@rockefeller.edu

M.J. Davey's present address is The University of Western Ontario, London, Ontario N6A 5B8, Canada.

Abbreviations used in this paper: ChIP, chromatin immunoprecipitation; MS, mass spectrometry; PrA, protein A.

The online version of this article includes supplemental material.

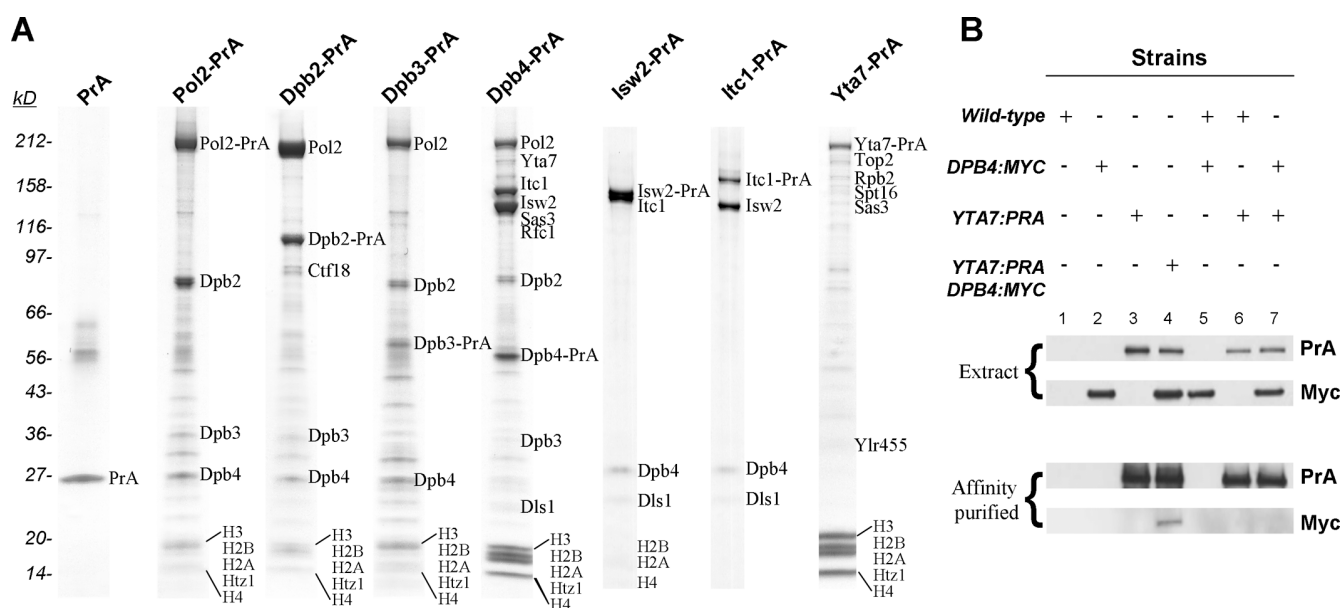


Figure 1. **Dpb4 forms multiple stable complexes with chromatin.** (A) Complexes were isolated via a PrA tag under conditions that copurified interacting proteins. These proteins were resolved by SDS-PAGE, visualized by Coomassie blue staining, and excised for MS identification. Labels show specific interactions with the PrA-tagged proteins. Reciprocal purifications of tagged members of the complexes demonstrated coisolation of Dpb4 with the exception of tagged Yta7. (B) Coimmunoprecipitation experiments with Yta7 and Dpb4 indicated that they associate in vivo. Note lane 7, which controls for post-lysis association of Yta7 and Dpb4 in vitro.

limitation of biochemical studies of chromatin-associated protein complexes is that in the absence of fixation they are usually isolated without their cognate DNA and nucleosomes. Therefore, it is essential to develop methods whereby chromatin-associated protein complexes can be isolated intact with their cognate DNA and nucleosomes, all in analyzable quantities. We have therefore assembled a suite of techniques that can yield microgram quantities of such intact chromatin complexes. We have used these techniques to identify and characterize a set of protein complexes that we found to bind discrete regions of the genome, certain of which are known boundaries between silent and active chromatin states. We have also shown that these complexes are important for the faithful maintenance of an established boundary as disruption of the complexes results in specific, anomalous alterations of the silent and active epigenetic states.

Results

Isolating intact chromatin complexes

To identify protein complexes involved in chromatin maintenance and propagation, we isolated numerous known chromatin-associated proteins, genomically tagged with protein A (PrA), under conditions that were sufficiently gentle to maintain interactions with other cellular macromolecules (Aitchison et al., 1995, 1996; Rout et al., 1997, 2000; unpublished data). Mass spectrometric identification of coisolating proteins (followed by exclusion of nonspecifically binding proteins as judged by their presence in immunisolations of 29 different chromatin-binding proteins [Fig. S1, available at <http://www.jcb.org/cgi/content/full/jcb.200502104/DC1>]) allowed us to identify specific members of each complex (Rout et al., 2000; Gavin et al., 2002; Ho et al., 2002; Archambault et al., 2003, 2004).

During this broad screen (Fig. S1 A), we discovered a discrete set of chromatin-bound proteins comprising overlapping complexes with the common component, Dpb4 (Fig. 1, Fig. S1 B, and Table S1, available at <http://www.jcb.org/cgi/content/full/jcb.200502104/DC1>). This set contained the DNA pol ϵ holoenzyme (Pol2, Dpb2, Dpb3, Dpb4) (Hamatake et al., 1990; Araki et al., 1991; Navas et al., 1995; Dua et al., 1998; Ohya et al., 2000; Hubscher et al., 2002; Ohya et al., 2002; Osborn et al., 2002; Chilkova et al., 2003; Edwards et al., 2003; Iida and Araki, 2004), as well as the clamp loader subunits Ctf18 and Rfc1 (Hanna et al., 2001; Mayer et al., 2001; Jeruzalmi et al., 2002; Edwards et al., 2003). The set also contained several other chromatin-associated proteins: the chromatin remodeling proteins Itc1, Isw2, and Dls1 (as expected [Iida and Araki, 2004; McConnell et al., 2004]), as well as the AAA ATPase Yta7, the histone acetyltransferase Sas3 and its partner Spt16, the DNA topoisomerase Top2, an RNA polymerase core subunit Rpb2, an uncharacterized protein Ylr455 (which by virtue of its PWWP domain is also likely to bind DNA), the core histones (H2A, H2B, H3, and H4), and the histone variant Htz1 (H2A.Z; Goto et al., 1984; Myer and Young, 1998; John et al., 2000; Stec et al., 2000; Frohlich, 2001; Howe et al., 2001; Kent et al., 2001; Kassabov et al., 2002; Qiu et al., 2002; Fazio and Tsukiyama, 2003; Meneghini et al., 2003). In summary, these isolations yielded at least two Dpb4-containing complexes, the pol ϵ and chromatin remodeling complexes.

Elucidating the architecture of the pol ϵ and chromatin remodeling complexes

To dissect these nucleosome-bound subcomplexes, we used a strategy whereby we isolated each pol ϵ subunit from cells in which either *DPB3* or *DPB4* had been deleted, reasoning that

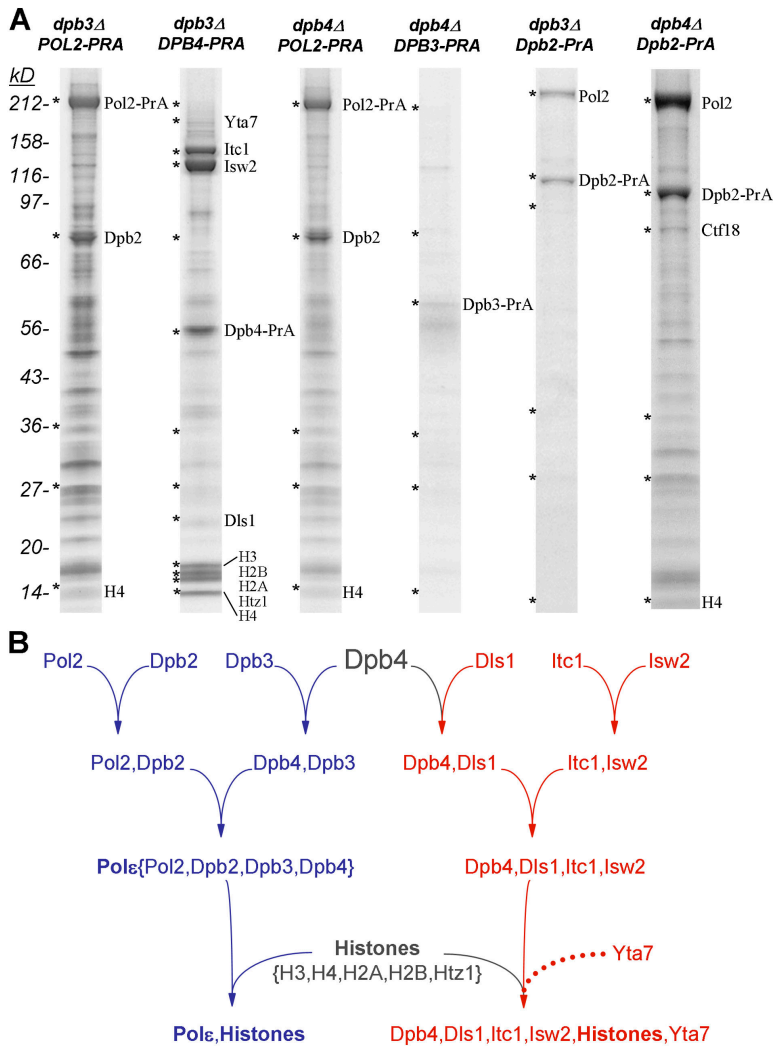


Figure 2. Elucidating the architecture of chromatin-associated complexes. (A) Dpb3 or Dpb4 was separately deleted in combination with the various PrA-tagged pol ϵ components. PrA-tagged components and their interacting proteins were isolated and visualized as for Fig. 1 A. Gel positions shown with asterisks, corresponding to the migration position of the proteins identified in Fig. 1, were excised and screened for the presence of these proteins by MS. (B) Proposed assembly pathway for chromatin complexes containing Dpb4.

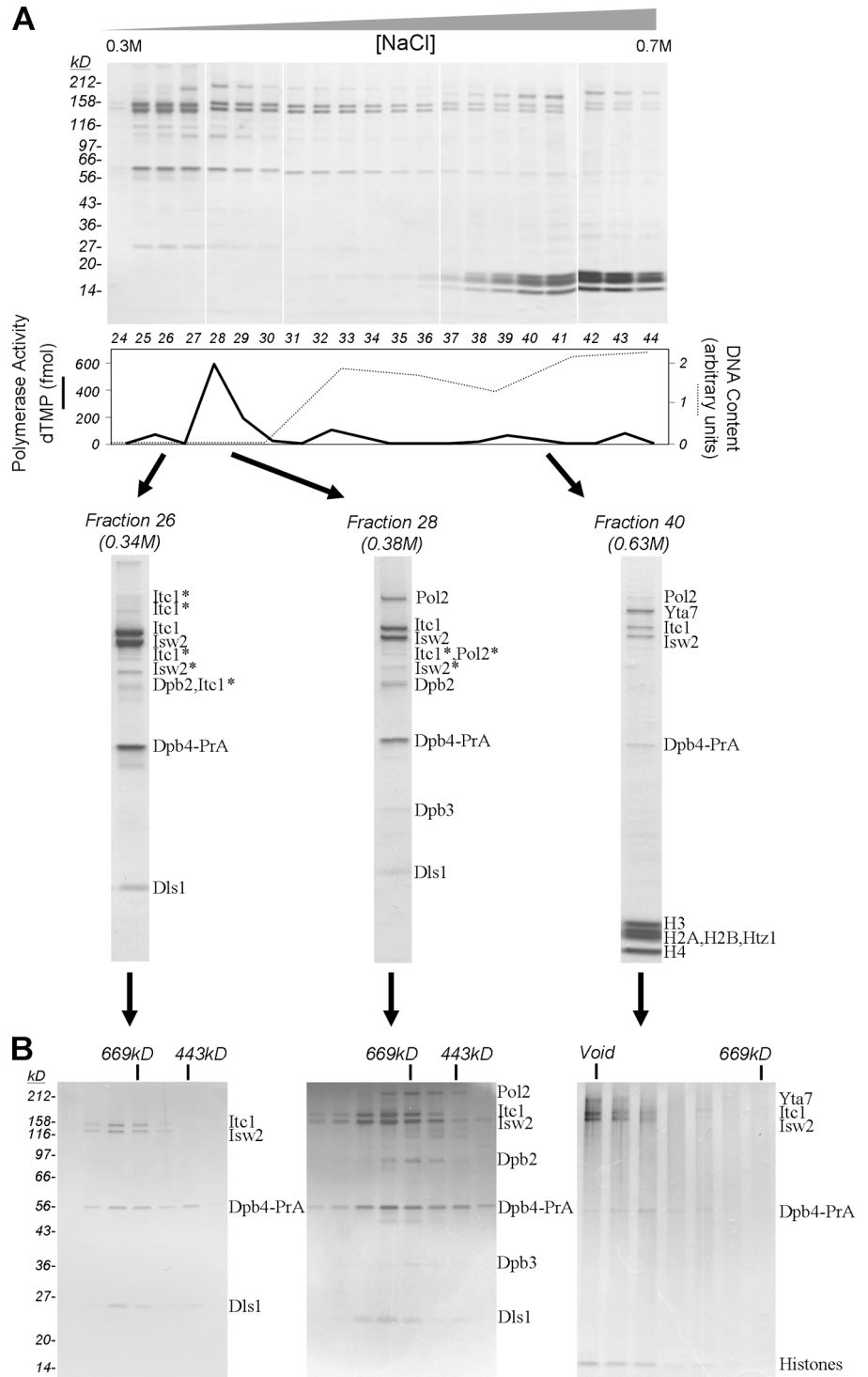
removal of a given component of pol ϵ could make the other interacting partners less stable (and so in principle provide information on the overall assembly of pol ϵ and associated complexes). To do this, we used a rapid “hypothesis-driven” mass spectrometric strategy to look for all major proteins detected in Fig. 1 (Kalkum et al., 2003). This strategy allowed us to determine the presence or absence of a protein with high sensitivity (Fig. 2 A).

Purification of Pol2-PrA in either the *dpb3Δ* or *dpb4Δ* background revealed that Pol2 interacts strongly with Dpb2 and that this pair of proteins associates with histones. Furthermore, Dpb3 and Dpb4 are codependent for association with the Pol2/Dpb2 pair because neither bound to Pol2-PrA or Dpb2-PrA in the absence of the other. These results are consistent with previous findings on interactions between the pol ϵ subunits (Dua et al., 2000). Purification of Dpb3-PrA in a *dpb4Δ* strain did not immunoprecipitate any additional components of pol ϵ , further confirming the codependence of Dpb3 and Dpb4 for association with the other components of the pol ϵ complex. Interestingly, immunopurification of Dpb4-PrA from a *dpb3Δ* strain yielded Itc1, Isw2, Yta7, Dls1, and histones, but did not immunoprecipitate any other member of the pol ϵ holoenzyme

(Fig. 2 A). Hence, Dpb4 interacts in separate pol ϵ and Dpb4/Itc1/Isw2/Dls1 complexes, which is consistent with previous data (Iida and Araki, 2004). However, we additionally observed that both complexes associate avidly with histones. The above-described dissection of these complexes allows us to propose their pathways of assembly, yielding at least two separate histone-associated complexes: one in which the histones are bound to chromatin remodeling proteins, and the other associated with the pol ϵ holoenzyme. This working hypothesis is presented in Fig. 2 B.

To further study the Dpb4-containing subcomplexes, we developed a semi-preparative purification strategy. This strategy uses PrA-affinity purification of the Dpb4-PrA complexes (~75 μ g), which after native elution from the affinity resin were separated by anion exchange chromatography. Three distinct Dpb4-containing fractions were resolved (Fig. 3 A). The first (fraction No. 26, 0.34 M [NaCl] eluate) contained the Dpb4-chromatin remodeling complex comprised of Itc1, Isw2, Dpb4-PrA, and Dls1. The second nearby eluting fraction (fraction No. 28, 0.38 M [NaCl]) contained the pol ϵ proteins Pol2, Dpb2, Dpb3, and Dpb4-PrA. Proteins in the 0.34 M [NaCl] eluate tailed into those in the 0.38 M [NaCl] eluate, although

Figure 3. Isolation of chromatin-associated protein complexes with their cognate DNA and histones. Complexes containing Dpb4-PrA were immunoprecipitated and eluted under nondenaturing conditions. (A) The eluate was loaded on an anion exchange column and fractions were collected from a 0–1 M [NaCl] gradient and visualized by Coomassie blue-stained SDS-PAGE. DNA polymerase activity was assayed by dTMP incorporation into calf thymus DNA. The presence of copurifying DNA was assayed by real-time PCR. Lanes containing three unique complexes are shown expanded, and the protein components identified by MS are labeled. Bands labeled with an asterisk may represent a breakdown product or alternate form of the protein. White lines indicate that intervening lanes have been spliced out. (B) The three unique complexes from A were further resolved by gel filtration. Fraction proteins were visualized by silver-stained SDS-PAGE.



the compositions of these fractions appear to be distinct. The third fraction (fraction No. 40, 0.63 M [NaCl]) contained Yta7, Itc1, Isw2, Dpb4, and the histones. Thus, the Dpb4-chromatin remodeling/histone complex identified in Fig. 1 was further resolved into the two salt-stable fractions at 0.34 and 0.63 M [NaCl]. The sub-stoichiometric levels of Dpb4 and Itc1/Isw2 with the Yta7-histone fraction are consistent with the low stoichiometry of Dpb4 in the Yta7-PrA pullout (Fig. 1, A and B). The individual fractions from the anion exchange separation

were assayed for polymerase activity *in vitro*, yielding a significant peak of activity in the fractions containing the Pol2 catalytic subunit of pol ϵ (Fig. 3 A). Given that we also identified clamp-loader proteins in association with the pol ϵ subunits (Fig. 1 A), we surmise that the pol ϵ holoenzyme is an active DNA polymerase *in vivo*.

Each of the three distinct fractions from the anion exchange column was found to contain stable subcomplex(es) by gel filtration (Fig. 3 B). Thus, the Itc1/Isw2/Dpb4-PrA/Dls1 complex ap-

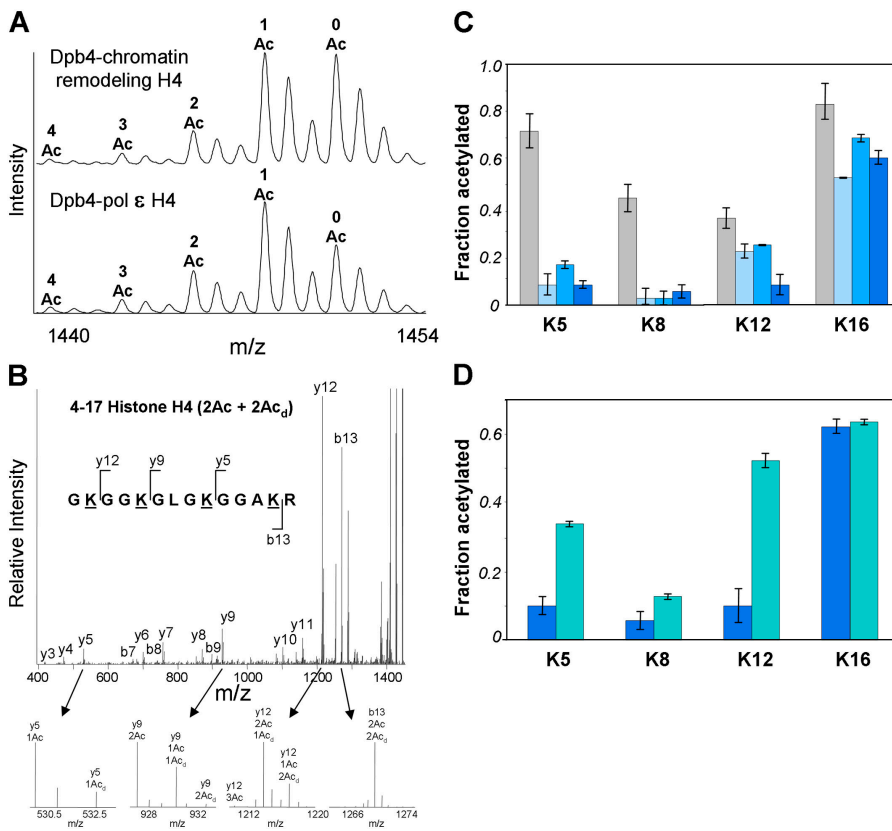


Figure 4. Pol ϵ and the chromatin-remodeling complexes are associated with a specific epigenetic state of chromatin. Histones from the Dpb4-chromatin remodeling complex and from the Dpb4-pol ϵ complex were PrA-affinity purified from *DPB4-PrA dpb3Δ* and *DPB3-PrA* strains, respectively. Histone H4 was modified in-gel with D₃-acetic anhydride to convert free lysines to D₃-acetyl lysines and then digested with trypsin. (A) MALDI-QqTOF mass spectrum of the tryptic peptide encompassing amino acid residues 4–17 of the NH₂-terminal tail of histone H4. All five possible acetylation states are labeled. (B) Each peptide ion species observed in A was fragmented in a MALDI-ion trap MS. The resulting heavy and light fragment ion intensities were used to determine the levels of acetylation on specific lysines. Shown is a representative fragmentation spectrum of peptide 4–17 containing two heavy (Ac_d) and two light (Ac) acetylations. The b- and y-fragment ions used to quantitate the levels of acetylation on each of the four lysines are shown expanded. (C) Site-specific levels of acetylation on histone H4 peptide 4–17 from global histones (gray), Dpb4-chromatin remodeling complex-associated histones (light blue), pol ϵ -associated histones from Dpb3-PrA immunoprecipitation (medium blue), and pol ϵ -associated histones from Pol2-PrA immunoprecipitation (dark blue). (D) Site-specific levels of acetylation on histone H4 peptide 4–17 from immunoprecipitation of Pol2-PrA (dark blue) and Pol2-PrA in *dpb3Δ* strain (green).

peared to form a multimer, as previously observed (Iida and Araki, 2004). Additionally, we observed a smaller subcomplex of Dpb4-PrA/Dls1 at ~443 kD, suggesting a multimeric interaction of these two components. Pol ϵ holoenzyme (Pol2, Dpb2, Dpb3, and Dpb4-PrA) eluted at a mass that was consistent with a heterodimer (Dua et al., 2000; Iida and Araki, 2004), and its elution was distinct from the Itc1/Isw2/Dpb4-PrA/Dls1 complex. The Yta7/Itc1/Isw2/Dpb4-PrA/histone complex was too large to be resolved, indicating purification of an extremely large entity containing DNA-protein nucleosome associations.

Both pol ϵ and the chromatin remodeling complexes are associated with a specific epigenetic state of chromatin

Histones can be posttranslationally modified by a series of specialized enzymes. Specific posttranslational modifications on histones have been correlated with either actively transcribed or repressed regions of chromatin (for reviews see Rusche et al., 2003; Vermaak et al., 2003). In particular, differential acetylation of histones has proven an important indicator of the transcriptional state of their associated chromatin (Kurdistani et al., 2004). One example is the acetylation or deacetylation of K5, K8, K12, and K16 of histone H4, which has been correlated with active or silent chromatin, respectively (Braunstein et al., 1996). Hence, we determined the absolute acetylation levels of lysines 5, 8, 12, and 16 in the histone H4 associated with the pol ϵ complex and the chromatin remodeling complex, comparing these levels with the histone H4 associated globally with yeast chromatin. We affinity purified the histones that were specifi-

cally associated with pol ϵ by using Dpb3-PrA (which exclusively pulls out the holoenzyme [Fig. 1 A]), whereas we affinity purified the chromatin-remodeling complex-associated histones by using Dpb4-PrA in a *dpb3Δ* strain (which exclusively pulls out the Dpb4-chromatin remodeling complex [Fig. 2 A]). These isolations were performed in the presence of sodium butyrate to inhibit histone deacetylases (Waterborg, 2000; unpublished data). To determine the degree of histone modification, we adapted an assay to measure acetylation states, using electrospray ionization mass spectrometry (MS) as the readout for use with MALDI MS (C.M. Smith et al., 2002, 2003).

After tryptic digestion, the four potential sites of histone H4 acetylation (K5, K8, K12, and K16) were all found in a peptide stretching from amino acid residues 4 to 17, which we term the 4–17 peptide. The 4–17 peptides from both pol ϵ and the chromatin remodeling complex were mostly either completely unacetylated or just singly acetylated, although low levels of doubly, triply, and quadruply acetylated peptide were also present (Fig. 4 A). To determine the degree of acetylation of the individual sites in each of these five peptide species, we collected MS² data (Fig. 4 B). Both pools of histone H4 were hypoacetylated at K5, K8, and K12 relative to global histone H4, whereas the levels of acetylation at K16 were more comparable to those observed in global histone H4 (Fig. 4 C). We found the same pattern of acetylation on histone H4 regardless of whether the pol ϵ -histone complex was isolated with Pol2-PrA or Dpb3-PrA (Fig. 4 C).

In summary, the same pattern of histone H4 acetylation is found in both pol ϵ and the chromatin remodeling complex.

Conversely, elimination of components of pol ϵ produced dramatic changes in the observed pattern of histone H4 acetylation; we infer that pol ϵ from the *dpb3 Δ* strain binds sites on chromatin that are differently modified than the normal pol ϵ sites, suggesting mislocalization of the polymerase (Fig. 4 D).

Hypoacetylation has classically been correlated with silent chromatin (Fischle et al., 2003), with a requisite for the binding of the Sir silencing proteins being hypoacetylation at K16 of histone H4 (Suka et al., 2002). Here, we observed a high level of acetylation at K16. This combination of both hypo- and hyperacetylation seems to be a blend of open and closed chromatin marks. We observed a similar combination of open and closed chromatin marks on histone H3; measurements of modifications on histone H3 isolated from both complexes revealed hypoacetylation of K9, K14, K18, K23, K27, and K56 (characteristic of silent chromatin) and \sim 80% mono-, di-, and trimethylation of K79 (characteristic of euchromatin because Sir binding requires hypomethylated H3 K79; van Leeuwen et al., 2002; Fig. S2, available at <http://www.jcb.org/cgi/content/full/jcb.200502104/DC1>).

To summarize, both pol ϵ and the Dpb4-chromatin remodeling complex bind distinctively and similarly modified histones, indicating that the complexes may bind to similar types of chromatin. The specifically modified histones that we found associated with these complexes was an average measurement of locations throughout the genome, and therefore reveals a preferential histone binding state for the pol ϵ and Dpb4-chromatin remodeling complexes. Therefore, we sought to determine where the Dpb4-associated complexes bind on the genome.

Genome-wide localization of Dpb4-associated complexes

The long retention times of the Dpb4-histone complexes on the anion exchange column (Fig. 3 A) indicated that these complexes were negatively charged overall. Because histones are positively charged, we surmised that a significant amount of negatively charged DNA was still present. Indeed, further investigation using PCR of each anion exchange fraction showed that DNA was specifically associated with the Dpb4-histone complexes (Fig. 3 A). Because the first step in our purification strategy is a DNase I treatment, this copurifying DNA must be tightly bound. This protected DNA was isolated, amplified by ligation-mediated PCR, and fluorescently labeled for DNA microarray analysis. The average length of the DNA protected in the Dpb4-histone complex was \sim 200 bp (unpublished data), which is on the order of a single nucleosome. Complexes isolated using DNA shearing instead of the DNase I treatment gave essentially the same result (unpublished data).

We localized the genomic positions of the Dpb4-histone-associated DNA by hybridization of the Dpb4-associated DNA to an intergenic DNA microarray of the *S. cerevisiae* genome. We observed enrichments at numerous discrete sites along the yeast chromosomes, with a tendency for clustering (summarized in Fig. 5 A; for the full data set of all the chromosomes see Table S2). Notably, the Dpb4-associated DNA was found to be particularly enriched toward most chromosome ends (proximal to the telomeres; Fig. 5, A and B). Several functionally related

genes families are found in these telomere proximal regions. We observed a high number of Dpb4-binding sites immediately adjacent to certain of these functionally related genes. For example, binding was found adjacent to all seven related members of the flocculation (*FLO*) gene family (*FLO1*, *FLO5*, *FLO8*, *FLO9*, *FLO10*, *FLO11*, *FIG2*; Fig. 5 A; Halme et al., 2004; Verstrepen et al., 2004). The Dpb4 complexes also flank other known stress response genes such as the *PAU* loci (anaerobic stress; Rachidi et al., 2000). It seems significant that the Dpb4 complex binding occurs next to families of genes that are known to be heterochromatically silenced and epigenetically controlled. In this context, we note that sites adjacent to the silent mating loci (*HML* and *HMR*) on chromosome III, canonical silent regions surrounded by active chromatin, were among the strongest binding sites for Dpb4 complexes (Fig. 5 C). Specifically, the complexes were preferentially associated with the well-defined right hand boundary element of *HMR* at (*tT(AGU)C*) as well as the less well-defined left hand boundary element (overlapping with or close to *YCR095C*) of *HMR*, which are areas of chromatin that prevent the heterochromatin covering *HMRA1* and *HMRA2* from spreading into surrounding euchromatic regions (Donze et al., 1999; Donze and Kamakaka, 2001; Lieb et al., 2001). This preferential enrichment with the boundary elements was confirmed with high resolution PCR mapping at *HMR* (Fig. 5 C) as well as with conventional ChIP-chip analysis (Fig. S3, available at <http://www.jcb.org/cgi/content/full/jcb.200502104/DC1>). At the *HML* locus, we observe the Dpb4 complexes to be preferentially associated with DNA spanning the region between *HML-I* and *CHAI* and (to a lesser extent) on the telomere side of *YCL073C* (Bi et al., 1999; Lieb et al., 2001). We conclude from these results that the Dpb4-associated complexes bind preferentially to particular chromatin regions, some of which are associated with known boundaries or with variegated epigenetic states.

Dpb4-associated complexes are required for the maintenance of a boundary state

To investigate the functional consequences of the association between the Dpb4-histone complexes and the boundary elements, we tested whether particular components of either pol ϵ holoenzyme (i.e., Dpb4, Dpb3) or the Dpb4-chromatin remodeling complex (i.e., Dpb4, Yta7, Sas3, Itc1, Isw2, and Dls1) play a role in the epigenetic regulation of the *HMR* locus. Specifically, we assayed strains carrying deletions of these proteins, as well as *HTZ1* and the control *SIR3*, for the expression of a *URA3* reporter gene placed in the following three locations: in the Sir-silenced region of *HMR*, at the left-hand boundary of *HMR*, and upstream of the boundary region (Donze et al., 1999). We assayed for silencing by duplicate plating of the strains on FOA and $-$ Ura. Consistent results were observed under both conditions; hence, for simplicity, we show only the FOA results in which an increased level of survival on FOA measures an increased level of *URA3* silencing (Fig. 6, A and B). As expected, removal of *SIR3* completely abolishes silencing (Donze et al., 1999; unpublished data). We evaluated how the deletions affected boundary maintenance by assaying the reporter strains both with and without *SIR3* plasmid.

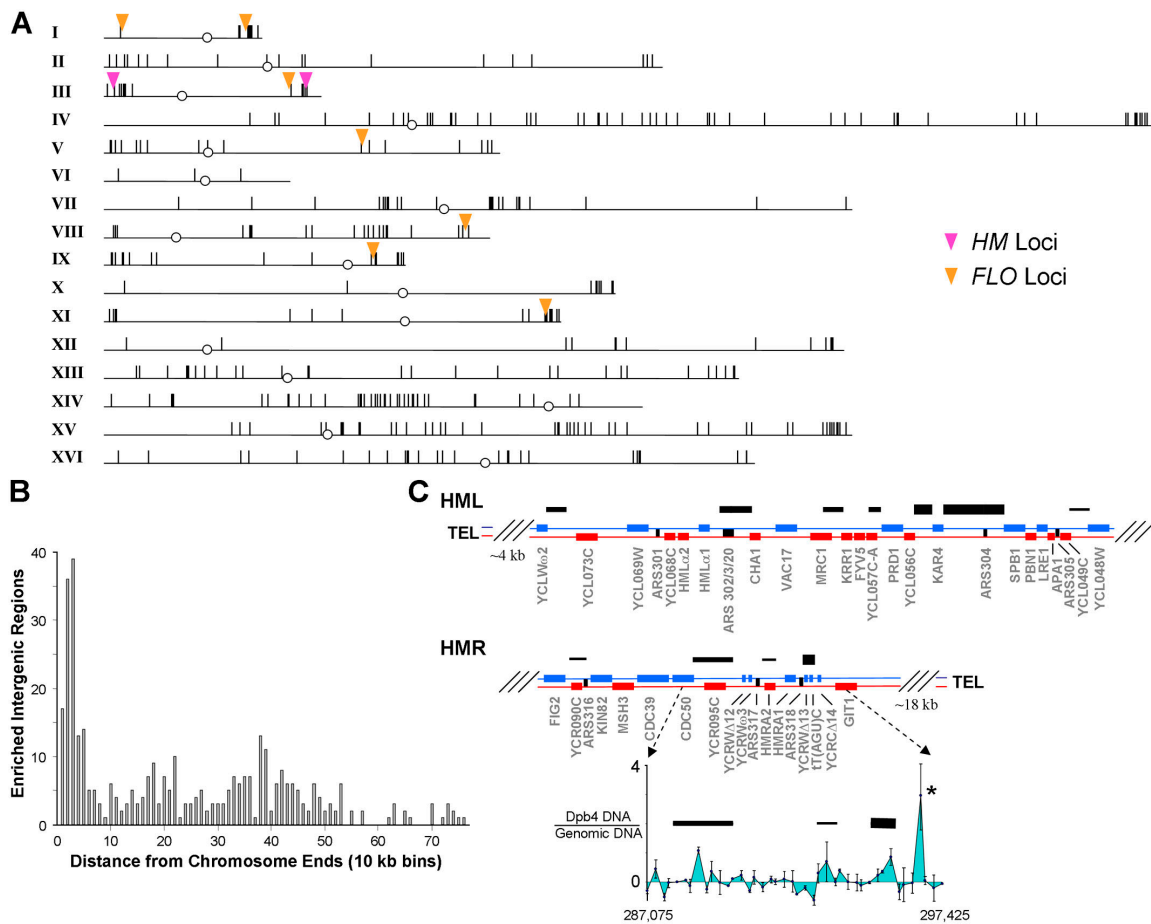


Figure 5. **Genome-wide localization of Dpb4-containing complexes.** Protected DNA from the purified fraction of Dpb4-associated histones in Fig. 3 A was hybridized to an intergenic DNA microarray covering the *S. cerevisiae* genome. (A) The sequences of chromosomes I–XVI are depicted as horizontal black lines with the centromeres denoted by circles. Vertical ticks indicate the position of sequences enriched with the Dpb4-histone complexes. The positions of two silenced gene clusters (*HM* and *FLO*) are indicated, showing their close apposition to the Dpb4-enriched sequences. (B) A histogram showing the number of intergenic regions enriched with the Dpb4-histone complexes is plotted as a function of distance from the chromosome ends. (C) Dpb4-histone complex DNA is enriched at boundaries to the silent, mating loci on chromosome III. Positions of enriched sequences are shown as horizontal black lines above the annotated chromosome with increasing line thickness indicating increasing enrichment. The inset shows high resolution mapping of Dpb4-enriched sequences from semiquantitative PCR analysis. The asterisk marks a region that was not covered by the microarray analysis.

In *WT* cells without additional Sir3, the reporter was silenced within the Sir-silenced region of *HMR*, but not at the boundary nor at the region adjacent to the boundary (Fig. 6 A, left; and Fig. 6 B, top). Silencing of the reporter was Sir3 dependent, because deletion of *SIR3* resulted in strong transcription in the formerly silenced zone (unpublished data). Addition of the *SIR3* plasmid in the *WT* cells induced a substantial increase in reporter silencing at the boundary as well as a modest increase of silencing at the proximal reporter (Fig. 6 A, right; and Fig. 6 B, top). Deletion of *HTZ1*, a variant of histone H2A, did not alter expression of the reporter at the LH boundary, consistent with a prior observation of no significant Sir spreading at the LH boundary (Meneghini et al., 2003)

In every case where an effect was observed with a deletion strain, the effect was strongest for the reporter placed close to the boundary (Fig. 6 B), further supporting the idea that the Dpb4-associated complexes functionally interact with this region. Deletion of components of the chromatin remodeling complex led to a dramatic increase in silencing at the boundary

reporter, demonstrating that these components are involved in maintaining the transcriptionally active state of regions adjacent to the silenced zones. Notably, this increase in silencing at the boundary was observed in the absence of the *SIR3* plasmid. When the *SIR3* plasmid was introduced into these same strains, no increase in silencing was observed. Apparently, the extra dose of Sir3 masks the enhanced silencing effect of deletion of the chromatin remodeling factors. The most dramatic increase in silencing at the boundary reporter was observed for *ya7 Δ* , indicating a role in the maintenance of active transcription near silent regions for this previously uncharacterized protein.

In contrast, removal of the pol ϵ protein Dpb3 appeared to produce a slight opposite effect; i.e., a slight depression of silencing within *HMR* (Fig. 6 B, top). Introduction of the *SIR3* plasmid into the *dpb3 Δ* strain considerably amplified this effect, yielding significant depression of Sir3-dependent silencing both within *HMR* and at the boundary (Fig. 6 B, bottom). We hypothesize that the loss of silencing over an extended region implies that pol ϵ is involved in maintaining and replicat-

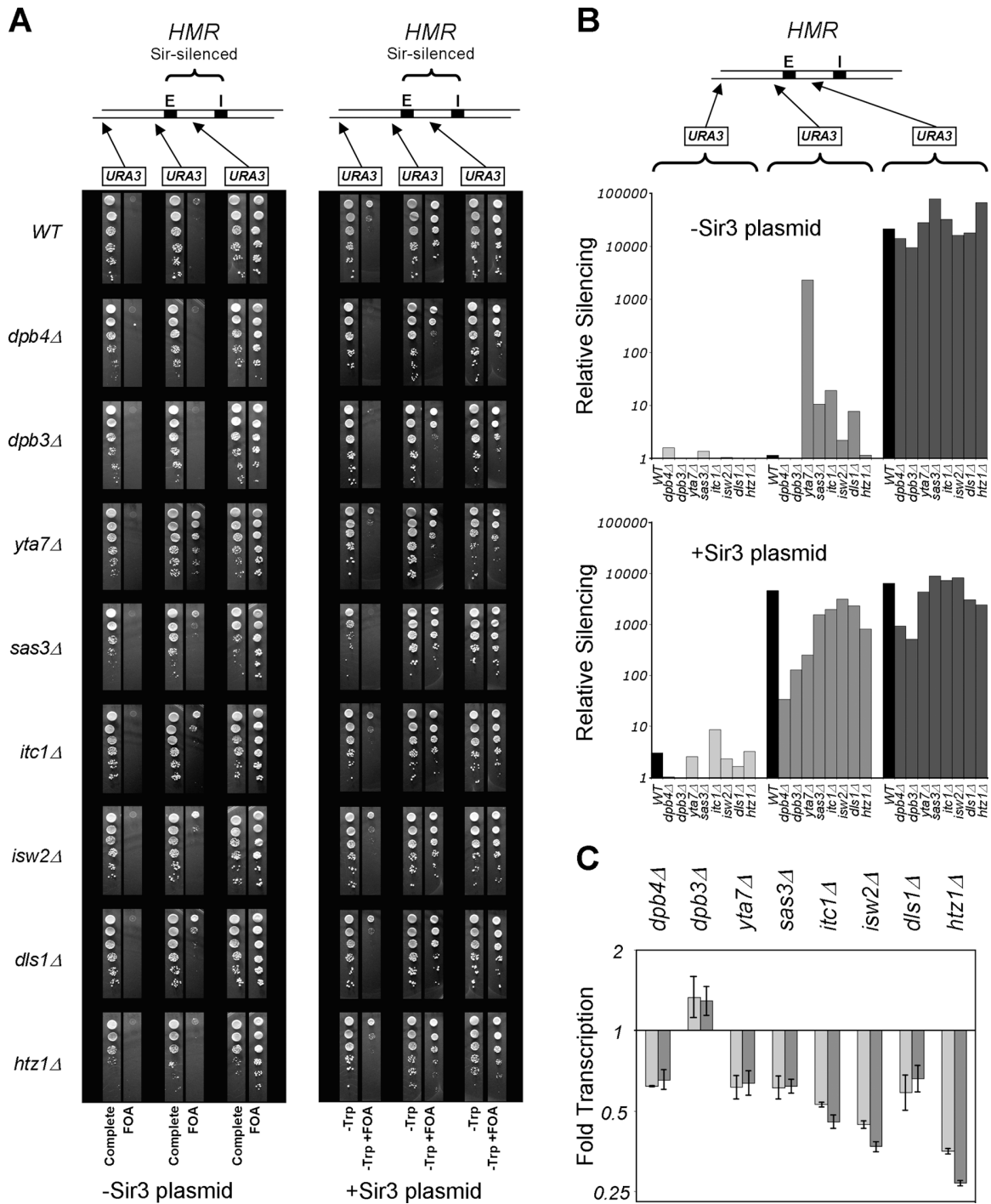


Figure 6. **Dpb4-containing chromatin complexes regulate an HMR boundary.** (A) Strains carrying deletions of *DPB4*, *DPB3*, *YTA7*, *SAS3*, *ITC1*, *ISW2*, *DLS1*, and *HTZ1* were assayed for the expression of a *URA3* reporter gene placed in the following three locations: in the Sir-silenced region of *HMR* (~640 bp to the right of *HMR-E*), at the left-hand boundary (~475 bp to the left of *HMR-E*), and within the *YCR095C* gene) (Donze et al., 1999). Decreased silencing of the reporter (i.e., increased transcription) results in increased cell death on FOA. Strains were assayed either without or with a Sir3-expressing plasmid. (B) Semiquantitative relative measure of the dilution-adjusted colony density seen in A. (C) Transcription levels of *YCR095C* (light gray) and *GIT1* (dark gray), genes proximal to *HMR*, were measured by real-time PCR. Fold transcription is relative to wild type. Measurements less than onefold indicate repression of transcription, whereas measurements greater than onefold indicate above normal transcription. Error bars show the SD of the mean for triplicate measurements.

ing the fully silent state of *HMR*. Deletion of Dpb4 exhibited a phenotype most resembling the deletion phenotype of the pol ϵ protein Dpb3 rather than that of the other members of the chromatin remodeling complex. This finding suggests that the pol

ϵ -related role of Dpb4 dominates its chromatin remodeling complex role in this assay.

As an alternative probe for alterations in boundary function, we measured deletion-dependent changes in mRNA levels

of two genes located adjacent to and on each side of the *HMR* (i.e., *GIT1* and *YCR095C*; Fig. 6 C). We observed reductions of transcription for members of the chromatin remodeling complex, but not the pol ϵ component Dpb3, again indicating a role for the chromatin remodeling complex in maintaining transcriptionally active regions at or near boundaries.

We also assayed for the loss of boundary function by measuring the occupancy of Sir3 within *HMR* relative to its occupancy of neighboring transcriptionally active zones in strains carrying the appropriate gene deletions (Meneghini et al., 2003). Thus, we performed ChIP assays on a region within the Sir-silenced *HMR* (*HMRA1*), at the left hand edge of *HMR*, at the adjacent genes *GIT1* and *YCR095C*, and in a region adjacent to the RH telomere of chromosome III. Although we observed a telomere-proximal effect for *htz1 Δ* as previously reported (Meneghini et al., 2003), we did not observe any statistically significant increase in Sir3 occupancy on the neighboring *GIT1* and *YCR095C* genes or at the edge of the *HMR* for *dpb4 Δ* , *dpb3 Δ* , *sas3 Δ* , *itc1 Δ* , *isw2 Δ* , *dls1 Δ* , and *htz1 Δ* (Fig. S4, available at <http://www.jcb.org/cgi/content/full/jcb.200502104/DC1>). These findings are in concert with our observations in the *URA3* reporter studies where, in the absence of the *SIR3* plasmid, we also observed relatively modest changes within the *HMR* and no discernible changes at *YCR095C*.

Despite the inherent vagaries associated with these different assays (and subtle phenotypic differences between each assay), they all pointed toward the involvement of both the pol ϵ and chromatin remodeling complexes in the faithful maintenance and propagation of the zone of transition between the silent and active states.

Dpb3 and Dpb4 are required for proper localization of pol ϵ to chromatin during DNA replication

Because Dpb3 is part of the Dpb4-pol ϵ complex, and its deletion caused a defect in the maintenance of silencing, we tested whether or not pol ϵ remained associated with the uniquely modified histones in a *dpb3 Δ* strain. Pol2-PrA was PrA-affinity purified from the *dpb3 Δ* strain and the acetylation on histone H4 was analyzed as described above (Fig. 4 D). Under these conditions, Pol2/Dpb2 was seen to associate with more acetylated histones than the uniquely modified histones, suggesting that Dpb3 (or the Dpb3/Dpb4 pair) is involved in localizing polymerase epsilon to the uniquely modified chromatin (Fig. 4 D).

Because pol ϵ is localized to boundary chromatin (Fig. 5), yet is an active DNA polymerase (Fig. 3 A) known to have a role in S phase (Ohya et al., 2002), we tested if this chromatin association was cell cycle dependent (Fig. 7 A). Although the four pol ϵ subunits maintained stable interactions with each other at each block, pol ϵ was associated with core histones only during times of DNA replication and segregation, indicating a cell cycle-dependent association of pol ϵ with chromatin. We also analyzed the acetylation state of the NH₂-terminal tail of histone H4 at the replication and mitosis blocks (Fig. 7 B). We observed that pol ϵ remained associated with the same unique type of modified histones during both blocks, display-

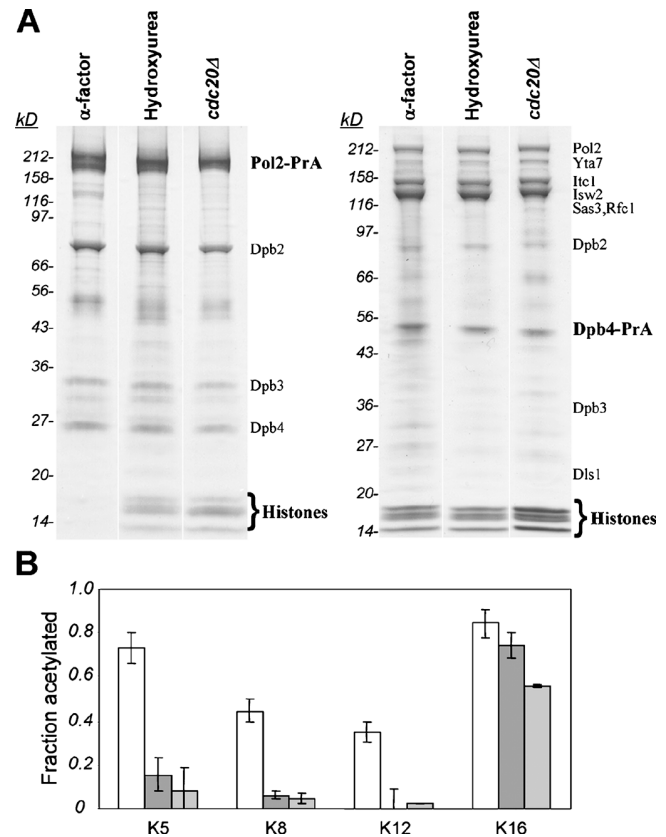


Figure 7. Pol ϵ associates with chromatin during DNA replication. (A) Pol2-PrA or Dpb4-PrA complexes were affinity purified at different cell cycle blocks, and their proteins were resolved by Coomassie blue-stained SDS-PAGE. White lines indicate that intervening lanes have been spliced out. (B) Site-specific levels of acetylation on histone H4 peptide 4–17 from the Pol2-PrA-associated histones from global (open), hydroxyurea block (dark gray), and *cdc20 Δ* block (light gray).

ing hypoacetylation on K5, K8, and K12 and relatively higher levels of acetylation on K16. This pattern is almost identical with that observed for pol ϵ -associated histones from the asynchronous cultures (Fig. 4 C), suggesting that pol ϵ is targeted to the same unique state of chromatin in a cell cycle-dependent manner. In contrast to the pol ϵ targeting, the Dpb4-containing chromatin remodeling complex remained associated with chromatin before and during times of DNA replication (Fig. 7 A), indicating a decoupling of the Dpb4-containing pol ϵ and chromatin remodeling complexes.

Discussion

We have dissected specialized assemblies on the *S. cerevisiae* genome that help define and preserve the boundaries that separate silent and active chromatin. These assemblies contain characteristic stretches of DNA that flank particular regions of silent chromatin, as well as five distinctively modified histones and a specific set of protein complexes. At least one of these complexes (pol ϵ) associates dynamically with this specialized chromatin, attaching in a cell cycle-dependent manner. Furthermore, we have shown that these complexes are important for the faithful maintenance of an established

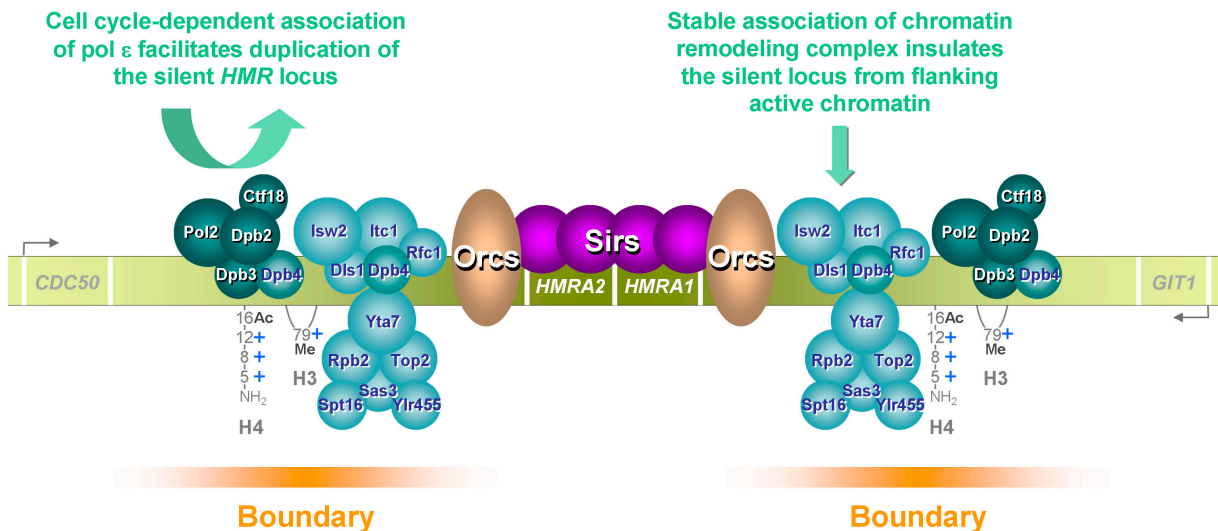


Figure 8. **A model for the roles of the Dpb4-associated complexes at a chromatin boundary.** The mating genes at *HMR* are contained within a region flanked by Orc complexes and transcriptionally silenced through the binding of Sir proteins. The Dpb4-containing pol ϵ and chromatin modifying/remodeling complexes associate with boundary regions where they bind distinctively modified histones. The pol ϵ complex aids in duplication of the silent chromatin, whereas the Dpb4-chromatin remodeling complex preserves the boundaries. Precise protein positions and their oligomeric states have not been determined.

boundary at *HMR*, because their disruption results in characteristic, anomalous alterations of certain silent and active epigenetic states. Because we isolate the Dpb4 complexes from whole cell lysates (rather than individual genomic loci), our protein composition and histone modification measurements represent an average of their preferential chromatin-bound states on many locations throughout the genome. Nevertheless, this represents, to our knowledge, the first report of the composition of protein complexes that are specifically associated with a boundary DNA sequence. In addition, we have defined a characteristic histone modification pattern associated with these complexes (Fig. 4).

Our findings support a multifunctional role for the Dpb4-containing pol ϵ and Dpb4-chromatin remodeling complexes at *HMR* (Fig. 8). We suggest that duplication of the silent state is aided by association of pol ϵ with the silent region during times of DNA replication (Fig. 7 A); alterations in the composition of pol ϵ , such as deletion of *DPB3*, result in mislocalization of the polymerase (Fig. 4 D) and inefficient replication of the silent state (Fig. 6, A and B). The duplication defect associated with removing Dpb3 from pol ϵ appears to be dependent on the amount of silent chromatin that needs to be duplicated. We speculate that normally partially mislocalized pol ϵ can still operate because WT levels of silent chromatin evidently do not overwhelm the polymerase. However, when the amount of silent chromatin is significantly increased by excess Sir3, the duplication capacity of the mislocalized polymerase becomes overwhelmed (Fig. 6, A and B). Correct propagation of the silent state also requires the maintenance of boundaries that separate transcriptionally active and silent chromatin. The chromatin remodeling complex, which remains associated with chromatin throughout the cell cycle (Fig. 7 B), appears to help maintain these boundary regions, preventing spreading of the silent state beyond the boundaries and into transcriptionally active regions (Fig. 6). Thus, the cell

appears to use two functionally different systems, coordinated at similar locations, to provide for propagation and maintenance of silent chromatin. Moreover, these boundary complexes have dual “yin-yang” roles; they preserve both the silent state of the chromatin within the boundaries and the active state of the chromatin outside of the boundaries.

In addition to *HMR* and *HML*, we observed enrichments of the complexes toward (but not exclusively at) most chromosome ends (Fig. 5, A and B). We observed a high number of Dpb4-binding sites immediately adjacent to certain functionally related genes. For example, binding was found adjacent to all seven related members of the *FLO* gene family (*FLO1*, *FLO5*, *FLO8*, *FLO9*, *FLO10*, *FLO11*, *FIG2*; Fig. 5 A). It is supposed, based on experiments, that these genes are expressed in response to various environmental stresses resulting in dramatically altered cell–cell and cell–substrate adhesion behavior. These genes are known to be normally silenced, but are epigenetically controlled in response to stress when subpopulations of cells in a colony switch from a *FLO*-silenced to a *FLO*-active state (Halme et al., 2004; Verstrepen et al., 2004). The Dpb4 complexes also flank other known stress response genes such as the *PAU* loci (anaerobic stress), which likewise are regulated by stochastic switching of their epigenetic state (Rachidi et al., 2000). It seems significant that the Dpb4 complex binding occurs next to families of genes that are known to be heterochromatically silenced and epigenetically controlled. These genes will be the subject of our future studies.

The data presented here lay a framework for further elucidation of the mechanisms by which cells establish, maintain, and transfer epigenetic information. The present focused proteomic and genomic approach enables comprehensive analyses of chromatin-associated protein complexes with their cognate DNA and nucleosomes and should be useful for further definition of chromatin structure and function.

Materials and methods

Strains and purification of PrA-tagged complexes

S. cerevisiae strains produced by homologous recombination are listed in Table S3. Growth conditions, cell lysis (2×10^{10} cells), cell cycle blocks (α -factor and *cdc20Δ*), purification of protein complexes using 3.75 mg of IgG-coated Dynabeads per gram of lysed cells, coimmunoprecipitation of PrA- and Myc-tagged proteins, and MS identification of proteins were largely as reported (Archambault et al., 2003). Cell cycle arrest during DNA replication was performed by addition of hydroxyurea (0.2 M).

Lysed cells were suspended in purification buffer (20 mM Hepes, pH 7.4, 0.1% Tween-20, 2 mM MgCl₂, 300 mM NaCl, 0.2 mg/ml PMSF, and 4 μg/ml pepstatin A) at 1 g lysed cells ($\sim 2 \times 10^{10}$ cells) per 5 ml of purification buffer. Note that purifications used for acetylation measurements contained 50 mM Na-butyrate and 250 mM NaCl in purification buffer. Suspended lysate was treated with 0.002% DNase I (wt/vol) (Sigma-Aldrich) for 10 min at RT with agitation. All subsequent steps were performed at 4°C. Samples were homogenized by using a Polytron (Brinkmann, PT 10/35), and then agitated for 1 h. The soluble fraction was isolated by centrifugation at 1,877 g (Sorvall H-1000B) for 10 min. The supernatant was incubated with 3.75 mg of Dynabeads (Dyna) cross-linked to rabbit IgG (Cappel) per 2×10^{10} lysed cells with agitation. Dynabeads were collected with a magnet and washed five times with purification buffer. The PrA-tagged protein and copurifying proteins were eluted from the IgG-Dynabeads with 0.5 N NH₄OH/0.5 mM EDTA. The samples were frozen in liquid nitrogen and evaporated to dryness in a SpeedVac (Thermo Savant). Dried protein samples were dissolved in loading buffer (78 mM Tris-Cl, 0.003% Bromophenol blue, 24.9 mM Tris base, 6.25 mM TCEP, 12.5% glycerol, and 2.5% SDS) and heated to 95°C for 5 min. Iodoacetamide (25 mM) was added for 30 min at RT to modify reduced cysteines. Samples were resolved by SDS-PAGE with Novex 4–20% Tris-glycine polyacrylamide gels (Invitrogen). Proteins in the gel were visualized by colloidal Coomassie staining with Gel Code Blue (Pierce Chemical Co.).

Hypothesis-driven mass spectrometric detection of proteins

For the knockout analysis in Fig. 2, an alternate MS strategy for protein identification was used. Gel slices were excised at positions that corresponded to proteins identified in Fig. 1 (irrespective of whether a band was visible) and analyzed by MALDI-MS (Archambault et al., 2003). Because certain components of the pol ϵ protein complexes were absent in the knockout analysis (Fig. 2), we used hypothesis-driven MS to definitively ascertain the presence or absence of these components (Kalkum et al., 2003).

Semi-preparative purification of Dpb4-PrA complexes

Dpb4-PrA-containing complexes were isolated as described in the section Strains and purification of PrA-tagged complexes except with larger number of cells ($\sim 10^{12}$). Protein complexes were eluted under nondenaturing conditions with PrA elution peptide. Elution peptide (0.7 mg/ml) was added to the Dynabeads for 20 min at 4°C with agitation. The eluate was collected and the elution was repeated at 20-min intervals for 2 h with fresh aliquots of elution peptide. The first three eluates, containing >90% of the eluted protein complexes (~ 75 μg), were pooled. The complexes were resolved by anion exchange chromatography (MiniQ PC 3.2/3 column on a SMART System; Amersham Biosciences). The gradient for anion exchange was 0–1 M NaCl in 20 mM Hepes, pH 7.4, 0.1% Tween-20, and 2 mM MgCl₂. Fractions were screened for polymerase activity using an activated calf thymus DNA polymerase assay with α -[³²P] dTTP. Fractions were also screened for DNA content by TaqMan (Applied Biosystems) real-time PCR targeted to YCR095C. Samples from the anion exchange column that contained resolved complexes were analyzed by gel filtration with a Superose 6 column on a SMART system (Amersham Biosciences). The buffer for the gel filtration analysis was 20 mM Hepes, pH 7.4, 0.1% Tween-20, 2 mM MgCl₂, and 300 mM NaCl.

DNA microarray analysis

DNA microarray experiments were performed as described previously (Ren et al., 2000) from the DNA precipitation step to and including microarray hybridization and washing. The remaining stages of microarray analyses were performed as described for mRNA expression microarrays (J.J. Smith et al., 2002). The sample for microarray analysis was taken from fraction 43 collected from the anion exchange column (Fig. 3). Control DNA was obtained by sonication or DNase I treatment of genomic DNA. DNA samples were hybridized to *S. cerevisiae* intergenic DNA microarrays (Institute for Systems Biology).

Semiquantitative PCR

PCR primers were designed to amplify ~ 150 bp regions in chromosome III coordinates 287,000–297,500 at ~ 200 – 300 bp intervals (Table S4). Semiquantitative PCR was performed in the linear amplification range for DNA used for hybridization to the intergenic microarrays and for control genomic DNA.

URA3 silencing assay

Strains containing a *URA3* reporter at *HMR* (Fig. 6) were constructed by genomic deletions of indicated genes with a *KANMX4* cassette in parent strains ROY508, ROY513, and ROY648 (gifts from R. Kamakaka, National Institute of Child Health and Human Development, Bethesda, MD; Donze et al., 1999). When mentioned, the strains were transformed with plasmid pRO146 that expressed Sir3 (a gift from R. Kamakaka). Strains were grown to stationary phase, normalized, serially diluted in 10-fold increments, and incubated at 30°C for 2 d. Without the *SIR3* plasmid, cell growth was monitored on synthetic complete, minus uracil, or plus FOA plates. With the *SIR3* plasmid, cell growth was monitored on minus tryptophan, minus tryptophan/minus uracil, or minus tryptophan/plus FOA plates.

Measurement of transcription levels

Total RNA was prepared from BY4742 mat α strains via hot acidic phenol extraction: wild-type, *dpb4Δ*, *dpb3Δ*, *yta7Δ*, *sas3Δ*, *itc1Δ*, *isw2Δ*, *dls1Δ*, and *htz1Δ*. Contaminant DNA was removed with the RNase-Free DNase Set (QIAGEN). cDNA was synthesized with the TaqMan Reverse Transcription Reagents Kit (Applied Biosystems). Transcription levels of *GIT1* relative to *ACT1* were measured with real-time PCR using the TaqMan system (Applied Biosystems; Table S4).

Analysis of histone H4 acetylation

To determine the degree of acetylation of histone H4 from the pol ϵ and chromatin remodeling complexes (purified in the presence of 50 mM sodium butyrate to inhibit histone deacetylases), we adapted an acetylation assay that used ESI MS for use with MALDI MS (C.M. Smith et al., 2002, 2003). Histone H4 gel bands were treated with 30% D₂-acetic anhydride (Cambridge Isotopes) in 100 mM ammonium bicarbonate (ABC) for 1 h at RT with constant agitation. This reaction converts unmodified lysine residues into D₃-acetyl-Lysines. Gel bands were washed with 100 mM ABC, dehydrated in acetonitrile, and rehydrated in 50 mM ABC containing 75 ng of trypsin (Roche). After digestion at 37°C for 6 h, peptides were crystallized in 2,5-dihydroxybenzoic acid for MALDI-MS (Archambault et al., 2003).

Mass spectra of digested histone H4 were obtained by MALDI-QqTOF MS (Krutchinsky et al., 2000). The intensities of the five possible combinations of heavy (Ac_D) and light (Ac) acetyls on the NH₂-terminal tail of histone H4 (amino acids 4–17) were determined (4 Ac, 3 Ac + 1 Ac_D, 2 Ac + 2 Ac_D, 1 Ac + 3 Ac_D, and 4 Ac_D). The intensity of a given monoisotopic peak (taken as a fraction of the total intensities of all monoisotopic peaks) represents the fractional population of that acetylated species. To obtain site-specific levels of acetylation, we acquired MS/MS spectra of each of the five species by MALDI-ion trap MS (Krutchinsky et al., 2001). Using previously published equations (Smith et al., 2003), adapted here for MALDI-MS, we measured the relative intensities of the y5, y9, y12, and b13 fragment ions to determine the relative acetylation levels of K16, K12, K8, and K5.

ChIP of Sir3-PrA

ChIP was performed in a similar manner as previously reported with the following modifications (Strahl-Bolsinger et al., 1997). Strains containing Sir3-PrA were grown to mid-logarithmic stage in triplicate and cross-linked with 1% formaldehyde for 10 min. After quenching the cross-linking with 125 mM glycine, cells were harvested by centrifugation, frozen in liquid nitrogen, and cryogenically broken with a Retsch type MM301 mixer mill. Broken cells were resuspended in ChIP buffer (50 mM Hepes, pH 7.5, 140 mM NaCl, 1 mM EDTA, 1% Triton X-100, 0.1% sodium deoxycholate, 0.2 mg/ml PMSF, and 4 μg/ml pepstatin A), and chromatin was sheared to an average size of 300 bp with sonication. After removal of cell debris by centrifugation, an aliquot (10%) was removed for ChIP input measurements. To the remainder we added IgG-coated Dyna beads for 1 h. Beads were washed sequentially with ChIP buffer, ChIP buffer supplemented with 360 mM NaCl, and 10 mM Tris-HCl (pH 7.4)/1 mM EDTA. The immunopurified ChIP sample was eluted from the beads by incubation at 65°C for 15 min in 50 mM Tris-HCl (pH 8.0)/10 mM EDTA/1% SDS. Cross-linking of the input and immunopurified ChIP samples was reversed at 65°C for 6 h. After proteinase K treatment, the DNA was isolated by phenol/chloroform extraction. The presence of DNA sequences from *HMRA1*, *GIT1*, *YCR095C*, and *ACT1* was detected with real-time PCR us-

ing the TaqMan system (Applied Biosystems). Triplicate PCR reactions were performed for each of the triplicate ChIPs. ChIP input samples were used to correct for variable primer efficiency. The background (*ACT1*) was subtracted from each immunopurified and input ChIP sample. The relative Sir3 abundance reflects the enrichment of *HMRA1*, *GIT1*, edge *HMR*, edge telomere, and *YCRO95C* sequences in the immunopurified ChIP samples relative to the ChIP input.

Online supplemental material

Fig. S1 shows Coomassie-stained gels showing representative immunoprecipitations of DNA replication complexes. Fig. S2 shows representative sections from a MALDI-QqTOF spectrum of tryptic peptides from histone H3 immunoprecipitated with Dpb4-PrA. Fig. S3 shows genome-wide localization of Dpb4 and Isw2 complexes. Fig. S4 shows ChIP of Sir3-PrA on the right end of chromosome III. Table S1 shows proteins identified by MALDI-MS in Fig. S1. Table S2 shows DNA microarray results from hybridization of Dpb4-histone DNA to an intergenic DNA microarray covering the *S. cerevisiae* genome (Fig. 5). Table S3 shows *S. cerevisiae* strains used in this study. Table S4 shows PCR primers used in this study. Online supplemental material is available at <http://www.jcb.org/cgi/content/full/jcb.200502104/DC1>.

We thank Titia de Lange, David Allis, Andrew Murray, Fred Cross, Jonathon Widom, Vincent Archambault, Sean Taverna, and Andrew Krutchinsky for enlightening discussions; members of the Rout and Chait laboratories for sharing their protocols and reagents; and Rohinton Kamakaka for yeast strains.

This work was supported by grants from the National Institutes of Health to B.T. Chait (RR00862), B.T. Chait and M.P. Rout (CA89810), A.J. Tackett (GM066496), and M. O'Donnell (GM38839). D.J. Dilworth acknowledges support from the Alberta Heritage Foundation for Medical Research and the Canadian Institute for Health Research, and J.D. Aitchison acknowledges support from Merck.

Submitted: 16 February 2005

Accepted: 3 March 2005

References

Aitchison, J.D., M.P. Rout, M. Marelli, G. Blobel, and R.W. Wozniak. 1995. Two novel related yeast nucleoporins Nup170p and Nup157p: complementation with the vertebrate homologue Nup155p and functional interactions with the yeast nuclear pore-membrane protein Pom152p. *J. Cell Biol.* 131:1133–1148.

Aitchison, J.D., G. Blobel, and M.P. Rout. 1996. Kap104p: a karyopherin involved in the nuclear transport of messenger RNA binding proteins. *Science*. 274:624–627.

Araki, H., R.K. Hamatake, A. Morrison, A.L. Johnson, L.H. Johnston, and A. Sugino. 1991. Cloning DPB3, the gene encoding the third subunit of DNA polymerase II of *Saccharomyces cerevisiae*. *Nucleic Acids Res.* 19:4867–4872.

Archambault, V., C.X. Li, A.J. Tackett, R. Wasch, B.T. Chait, M.P. Rout, and F.R. Cross. 2003. Genetic and biochemical evaluation of the importance of Cdc6 in regulating mitotic exit. *Mol. Biol. Cell.* 14:4592–4604.

Archambault, V., E.J. Chang, B.J. Drapkin, F.R. Cross, B.T. Chait, and M.P. Rout. 2004. Targeted proteomic study of the cyclin-cdk module. *Mol. Cell.* 14:699–711.

Becker, P.B., and W. Horz. 2002. ATP-dependent nucleosome remodeling. *Annu. Rev. Biochem.* 71:247–273.

Bi, X., and J.R. Broach. 2001. Chromosomal boundaries in *S. cerevisiae*. *Curr. Opin. Genet. Dev.* 11:199–204.

Bi, X., M. Braunstein, G.J. Shei, and J.R. Broach. 1999. The yeast HML I silencer defines a heterochromatin domain boundary by directional establishment of silencing. *Proc. Natl. Acad. Sci. USA.* 96:11934–11939.

Braunstein, M., R.E. Sobel, C.D. Allis, B.M. Turner, and J.R. Broach. 1996. Efficient transcriptional silencing in *Saccharomyces cerevisiae* requires a heterochromatin histone acetylation pattern. *Mol. Cell. Biol.* 16:4349–4356.

Burgess-Beusse, B., C. Farrell, M. Gaszner, M. Litt, V. Mutskov, F. Recillas-Targa, M. Simpson, A. West, and G. Felsenfeld. 2002. The insulation of genes from external enhancers and silencing chromatin. *Proc. Natl. Acad. Sci. USA.* 99:16433–16437.

Chilkova, O., B.H. Jonsson, and E. Johansson. 2003. The quaternary structure of DNA polymerase epsilon from *Saccharomyces cerevisiae*. *J. Biol. Chem.* 278:14082–14086.

Dhillon, N., and R.T. Kamakaka. 2002. Breaking through to the other side: si-

lencers and barriers. *Curr. Opin. Genet. Dev.* 12:188–192.

Donze, D., and R.T. Kamakaka. 2001. RNA polymerase III and RNA polymerase II promoter complexes are heterochromatin barriers in *Saccharomyces cerevisiae*. *EMBO J.* 20:520–531.

Donze, D., C.R. Adams, J. Rine, and R.T. Kamakaka. 1999. The boundaries of the silenced HMR domain in *Saccharomyces cerevisiae*. *Genes Dev.* 13:698–708.

Dua, R., D.L. Levy, and J.L. Campbell. 1998. Role of the putative zinc finger domain of *Saccharomyces cerevisiae* DNA polymerase epsilon in DNA replication and the S/M checkpoint pathway. *J. Biol. Chem.* 273:30046–30055.

Dua, R., S. Edwards, D.L. Levy, and J.L. Campbell. 2000. Subunit interactions within the *Saccharomyces cerevisiae* DNA polymerase epsilon (pol epsilon) complex. Demonstration of a dimeric pol epsilon. *J. Biol. Chem.* 275:28816–28825.

Edwards, S., C.M. Li, D.L. Levy, J. Brown, P.M. Snow, and J.L. Campbell. 2003. *Saccharomyces cerevisiae* DNA polymerase epsilon and polymerase sigma interact physically and functionally, suggesting a role for polymerase epsilon in sister chromatid cohesion. *Mol. Cell. Biol.* 23:2733–2748.

Fazio, T.G., and T. Tsukiyama. 2003. Chromatin remodeling in vivo: evidence for a nucleosome sliding mechanism. *Mol. Cell.* 12:1333–1340.

Fischle, W., Y. Wang, and C.D. Allis. 2003. Histone and chromatin cross-talk. *Curr. Opin. Cell Biol.* 15:172–183.

Frohlich, K.U. 2001. An AAA family tree. *J. Cell Sci.* 114:1601–1602.

Gavin, A.C., M. Bosche, R. Krause, P. Grandi, M. Marzioch, A. Bauer, J. Schultz, J.M. Rick, A.M. Michon, C.M. Cruciat, et al. 2002. Functional organization of the yeast proteome by systematic analysis of protein complexes. *Nature.* 415:141–147.

Goto, T., P. Laipis, and J.C. Wang. 1984. The purification and characterization of DNA topoisomerases I and II of the yeast *Saccharomyces cerevisiae*. *J. Biol. Chem.* 259:10422–10429.

Haber, J.E. 1998. Mating-type gene switching in *Saccharomyces cerevisiae*. *Annu. Rev. Genet.* 32:561–599.

Halme, A., S. Bumgarner, C. Styles, and G.R. Fink. 2004. Genetic and epigenetic regulation of the FLO gene family generates cell-surface variation in yeast. *Cell.* 116:405–415.

Hamatake, R.K., H. Hasegawa, A.B. Clark, K. Bebenek, T.A. Kunkel, and A. Sugino. 1990. Purification and characterization of DNA polymerase II from the yeast *Saccharomyces cerevisiae*. Identification of the catalytic core and a possible holoenzyme form of the enzyme. *J. Biol. Chem.* 265:4072–4083.

Hanna, J.S., E.S. Kroll, V. Lundblad, and F.A. Spencer. 2001. *Saccharomyces cerevisiae* CTF18 and CTF4 are required for sister chromatid cohesion. *Mol. Cell. Biol.* 21:3144–3158.

Ho, Y., A. Gruhler, A. Heilbut, G.D. Bader, L. Moore, S.L. Adams, A. Millar, P. Taylor, K. Bennett, K. Boutilier, et al. 2002. Systematic identification of protein complexes in *Saccharomyces cerevisiae* by mass spectrometry. *Nature.* 415:180–183.

Howe, L., D. Auston, P. Grant, S. John, R.G. Cook, J.L. Workman, and L. Pillus. 2001. Histone H3 specific acetyltransferases are essential for cell cycle progression. *Genes Dev.* 15:3144–3154.

Hubscher, U., G. Maga, and S. Spadari. 2002. Eukaryotic DNA polymerases. *Annu. Rev. Biochem.* 71:133–163.

Iida, T., and H. Araki. 2004. Noncompetitive counteractions of DNA polymerase epsilon and ISW2/yCHRAC for epigenetic inheritance of telomere position effect in *Saccharomyces cerevisiae*. *Mol. Cell. Biol.* 24:217–227.

Ishii, K., and U.K. Laemmli. 2003. Structural and dynamic functions establish chromatin domains. *Mol. Cell.* 11:237–248.

Jenuwein, T., and C.D. Allis. 2001. Translating the histone code. *Science.* 293:1074–1080.

Jeruzalmi, D., M. O'Donnell, and J. Kuriyan. 2002. Clamp loaders and sliding clamps. *Curr. Opin. Struct. Biol.* 12:217–224.

John, S., L. Howe, S.T. Tafrov, P.A. Grant, R. Sternglanz, and J.L. Workman. 2000. The something about silencing protein. Sas3, is the catalytic subunit of NuA3, a yTAF(II)30-containing HAT complex that interacts with the Spt16 subunit of the yeast CP (Cdc68/Pob3)-FACT complex. *Genes Dev.* 14:1196–1208.

Kalkum, M., G.J. Lyon, and B.T. Chait. 2003. Detection of secreted peptides by using hypothesis-driven multistage mass spectrometry. *Proc. Natl. Acad. Sci. USA.* 100:2795–2800.

Kassabov, S.R., N.M. Henry, M. Zofall, T. Tsukiyama, and B. Bartholomew. 2002. High-resolution mapping of changes in histone-DNA contacts of nucleosomes remodeled by ISW2. *Mol. Cell. Biol.* 22:7524–7534.

Kent, N.A., N. Karabetsov, P.K. Politis, and J. Mellor. 2001. In vivo chromatin

- remodeling by yeast ISWI homologs Isw1p and Isw2p. *Genes Dev.* 15: 619–626.
- Krutchinsky, A.N., W. Zhang, and B.T. Chait. 2000. Rapidly switchable matrix-assisted laser desorption/ionization and electrospray quadrupole-time-of-flight mass spectrometry for protein identification. *J. Am. Soc. Mass Spectrom.* 11:493–504.
- Krutchinsky, A.N., M. Kalkum, and B.T. Chait. 2001. Automatic identification of proteins with a MALDI-quadrupole ion trap mass spectrometer. *Anal. Chem.* 73:5066–5077.
- Kurdistani, S.K., S. Tavazoie, and M. Grunstein. 2004. Mapping global histone acetylation patterns to gene expression. *Cell.* 117:721–733.
- Labrador, M., and V.G. Corces. 2002. Setting the boundaries of chromatin domains and nuclear organization. *Cell.* 111:151–154.
- Laloraya, S., V. Guacci, and D. Koshland. 2000. Chromosomal addresses of the cohesin component Mcd1p. *J. Cell Biol.* 151:1047–1056.
- Lieb, J.D., X. Liu, D. Botstein, and P.O. Brown. 2001. Promoter-specific binding of Rap1 revealed by genome-wide maps of protein-DNA association. *Nat. Genet.* 28:327–334.
- Mayer, M.L., S.P. Gygi, R. Aebersold, and P. Hieter. 2001. Identification of RFC(Ctf18p, Ctf8p, Dcc1p): an alternative RFC complex required for sister chromatid cohesion in *S. cerevisiae*. *Mol. Cell.* 7:959–970.
- McConnell, A.D., M.E. Gelbart, and T. Tsukiyama. 2004. Histone fold protein Dls1p is required for Isw2-dependent chromatin remodeling in vivo. *Mol. Cell Biol.* 24:2605–2613.
- Meneghini, M.D., M. Wu, and H.D. Madhani. 2003. Conserved histone variant H2A.Z protects euchromatin from the ectopic spread of silent heterochromatin. *Cell.* 112:725–736.
- Mizuguchi, G., X. Shen, J. Landry, W.H. Wu, S. Sen, and C. Wu. 2004. ATP-driven exchange of histone H2AZ variant catalyzed by SWR1 chromatin remodeling complex. *Science.* 303:343–348.
- Myer, V.E., and R.A. Young. 1998. RNA polymerase II holoenzymes and subcomplexes. *J. Biol. Chem.* 273:27757–27760.
- Navas, T.A., Z. Zhou, and S.J. Elledge. 1995. DNA polymerase epsilon links the DNA replication machinery to the S phase checkpoint. *Cell.* 80:29–39.
- Ohya, T., S. Maki, Y. Kawasaki, and A. Sugino. 2000. Structure and function of the fourth subunit (Dpb4p) of DNA polymerase epsilon in *Saccharomyces cerevisiae*. *Nucleic Acids Res.* 28:3846–3852.
- Ohya, T., Y. Kawasaki, S. Hiraga, S. Kanbara, K. Nakajo, N. Nakashima, A. Suzuki, and A. Sugino. 2002. The DNA polymerase domain of pol(epsilon) is required for rapid, efficient, and highly accurate chromosomal DNA replication, telomere length maintenance, and normal cell senescence in *Saccharomyces cerevisiae*. *J. Biol. Chem.* 277:28099–28108.
- Oki, M., L. Valenzuela, T. Chiba, T. Ito, and R.T. Kamakaka. 2004. Barrier proteins remodel and modify chromatin to restrict silenced domains. *Mol. Cell Biol.* 24:1956–1967.
- Osborn, A.J., S.J. Elledge, and L. Zou. 2002. Checking on the fork: the DNA-replication stress-response pathway. *Trends Cell Biol.* 12:509–516.
- Qiu, C., K. Sawada, X. Zhang, and X. Cheng. 2002. The PWWP domain of mammalian DNA methyltransferase Dnmt3b defines a new family of DNA-binding folds. *Nat. Struct. Biol.* 9:217–224.
- Rachidi, N., M.J. Martinez, P. Barre, and B. Blondin. 2000. *Saccharomyces cerevisiae* PAU genes are induced by anaerobiosis. *Mol. Microbiol.* 35: 1421–1430.
- Ren, B., F. Robert, J.J. Wyrick, O. Aparicio, E.G. Jennings, I. Simon, J. Zeitlinger, J. Schreiber, N. Hannett, E. Kanin, et al. 2000. Genome-wide location and function of DNA binding proteins. *Science.* 290:2306–2309.
- Rout, M.P., G. Blobel, and J.D. Aitchison. 1997. A distinct nuclear import pathway used by ribosomal proteins. *Cell.* 89:715–725.
- Rout, M.P., J.D. Aitchison, A. Suprapto, K. Hjertaas, Y. Zhao, and B.T. Chait. 2000. The yeast nuclear pore complex: composition, architecture, and transport mechanism. *J. Cell Biol.* 148:635–651.
- Rusche, L.N., A.L. Kirchmaier, and J. Rine. 2003. The establishment, inheritance, and function of silenced chromatin in *Saccharomyces cerevisiae*. *Annu. Rev. Biochem.* 72:481–516.
- Smith, C.M., Z.W. Haimberger, C.O. Johnson, A.J. Wolf, P.R. Gafken, Z. Zhang, M.R. Parthun, and D.E. Gottschling. 2002. Heritable chromatin structure: mapping “memory” in histones H3 and H4. *Proc. Natl. Acad. Sci. USA.* 99:16454–16461.
- Smith, C.M., P.R. Gafken, Z. Zhang, D.E. Gottschling, J.B. Smith, and D.L. Smith. 2003. Mass spectrometric quantification of acetylation at specific lysines within the amino-terminal tail of histone H4. *Anal. Biochem.* 316: 23–33.
- Smith, J.J., M. Marelli, R.H. Christmas, F.J. Vizeacoumar, D.J. Dilworth, T. Ideker, T. Galitski, K. Dimitrov, R.A. Rachubinski, and J.D. Aitchison. 2002. Transcriptome profiling to identify genes involved in peroxisome assembly and function. *J. Cell Biol.* 158:259–271.
- Stec, I., S.B. Nagl, G.J. van Ommen, and J.T. den Dunnen. 2000. The PWWP domain: a potential protein-protein interaction domain in nuclear proteins influencing differentiation? *FEBS Lett.* 473:1–5.
- Strahl-Bolsinger, S., A. Hecht, K. Luo, and M. Grunstein. 1997. Sir2 and Sir4 interactions differ in core and extended telomeric heterochromatin in yeast. *Genes Dev.* 11:83–93.
- Suka, N., K. Luo, and M. Grunstein. 2002. Sir2p and Sas2p oppositely regulate acetylation of yeast histone H4 lysine16 and spreading of heterochromatin. *Nat. Genet.* 32:378–383.
- van Leeuwen, F., P.R. Gafken, and D.E. Gottschling. 2002. Dot1p modulates silencing in yeast by methylation of the nucleosome core. *Cell.* 109:745–756.
- Vermaak, D., K. Ahmad, and S. Henikoff. 2003. Maintenance of chromatin states: an open-and-shut case. *Curr. Opin. Cell Biol.* 15:266–274.
- Verstrepen, K.J., T.B. Reynolds, and G.R. Fink. 2004. Origins of variation in the fungal cell surface. *Nat Rev Microbiol.* 2:533–540.
- Waterborg, J.H. 2000. Steady-state levels of histone acetylation in *Saccharomyces cerevisiae*. *J. Biol. Chem.* 275:13007–13011.
- Zhang, Z., M.K. Hayashi, O. Merkel, B. Stillman, and R.M. Xu. 2002. Structure and function of the BAH-containing domain of Orc1p in epigenetic silencing. *EMBO J.* 21:4600–4611.